Applied Catalysis A: General 362 (2009) 88–94

Contents lists available at ScienceDirect

Applied Catalysis A: General

journal homepage: www.elsevier.com/locate/apcata

The effect of potassium addition to Pt supported on YSZ on steam reforming of mixtures of methane and ethane

Patrick O. Graf, Barbara L. Mojet, Leon Lefferts *

Catalytic Processes and Materials, IMPACT, University of Twente, PO Box 217, 7500 AE Enschede, The Netherlands

ARTICLE INFO

Article history:
Received 3 February 2009
Received in revised form 19 March 2009
Accepted 14 April 2009
Available online 18 April 2009

Keywords:
Platinum
Potassium
Steam reforming
Methane
Ethane
FT-IR CO adsorption

ABSTRACT

The influence of potassium addition on Pt supported on yttrium-stabilized zirconia (YSZ) was studied with FT-IR CO adsorption and CO-FT-IR-TPD, in order to understand the effect of potassium on the performance of the catalyst in reforming of mixtures of methane and ethane. Potassium modification of PtYSZ strongly influenced the conversion and rate determining steps in methane and ethane in steam reforming. Water activation is the rate determining step on PtYSZ, resulting in high surface coverage of hydrocarbon fragments during steam reforming of mixtures of methane and ethane. This led to blocking of active sites by ethane fragments and consequently low conversion of methane. If potassium is added to the catalyst, hydrocarbon activation on Pt is rate determining, resulting in low surface coverage of methane and ethane. As a result, competition effects of methane and ethane diminished on potassium modified PtYSZ, enabling simultaneous conversion of methane and ethane. The weakening of the interaction of the hydrocarbons with the Pt surface as a result of potassium addition is supported by the fact that the interaction with CO is weakened, as observed with FT-IR-TPD.

1. Introduction

Natural gas, mainly consisting of methane, is available in large quantities and is becoming one of the major resources for energy and chemicals. A new concept for utilization of methane has been proposed by us, as discussed in detail in earlier work [1,2]. Shortly, the intention is to combine oxidative coupling and inevitable combustion with reforming reactions of methane (Eqs. (1)–(4)) in one multifunctional autothermal reactor. This should lead to production of ethylene and synthesis gas in one autothermal process, in which the energy released in reactions (1) and (2) is used to reform methane through reactions (3) and (4).

$$CH_4 + (1/2)O_2 \rightarrow (1/2)C_2H_4 + H_2O, \qquad \Delta H_r = -140\,\text{kJ/mol} \quad (1)$$

$$CH_4 + 2O_2 \rightarrow CO_2 + 2H_2O, \qquad \Delta H_r = -801\,\text{kJ/mol} \quad (2)$$

$$CH_4 + H_2O \rightarrow 3H_2 + CO, \qquad \Delta H_r = 226\,\text{kJ/mol} \quad (3)$$

$$CH_4 + CO_2 \rightarrow 2H_2 + 2CO, \qquad \Delta H_r = 260\,\text{kJ/mol} \quad (4)$$

For the complete process, two catalysts are needed, one for oxidative coupling and other for the reforming reaction. This paper reports about the steam reforming step (3) of the mixture produced in the oxidative coupling, containing methane, ethane and ethylene. All these hydrocarbons are reactive in steam reforming [3]. The main challenge in this project is to prevent or limit the steam reforming of ethane and ethylene, while methane should be effectively converted.

Pt supported on zirconia proved to be a stable catalyst in steam and dry reforming of methane [4–7]. In earlier research [2], Pt supported on yttrium-stabilized zirconia (YSZ) was found to be the most suitable metal catalyst for steam reforming of single reactants. However, in mixtures of hydrocarbons methane conversion was suppressed by the presence of ethane or ethylene [1]. It also was demonstrated that the presence of potassium on PtYSZ (Pt4K700) prevents competition between methane and ethane during steam reforming and relatively more methane can be converted [1]. In accordance with literature [8–12], potassium modified catalysts initially showed low activity. Potassium modified catalysts activated with time on stream (TOS), which was attributed to partial evaporation of potassium during steam reforming. In the present paper, the characterization of the catalysts is discussed.

An easily accessible technique to study the surface properties of supported platinum catalysts is the adsorption of CO [13–15] (and references therein). The addition of potassium to noble metal catalysts is known to influence the electronic structure of the surface atoms via modification of the metal particle potential [16–20]. In turn, the electronic properties of the metal particle have been related to their catalytic properties in hydrogenolysis,

* Corresponding author. Tel.: +31 0534893033; fax: +31 0534894683.
E-mail address: L.Lefferts@utwente.nl (L. Lefferts).

0926-860X/$ – see front matter © 2009 Elsevier B.V. All rights reserved.
doi:10.1016/j.apcata.2009.04.022

hydrogenation and oxidation reactions [13–15,21]. Usually characterization studies are performed on small metal particles (few nanometers). However, in the present study, the relevant temperature window for steam reforming is between 700 and 800 °C, because of the integrated operation of reforming and oxidative coupling. This means that Pt particles are relatively large (10–100 nm); with the lower number of surface sites characterization becomes a challenging issue.

In this paper, reactivity of methane and ethane in steam reforming on PtYSZ and potassium modified PtYSZ is investigated and the catalysts are characterized with FT-IR spectroscopy. TPD of CO on unmodified PtYSZ and potassium modified PtYSZ is used to estimate trends in the adsorption strength of methane and ethane. In addition to the kinetic data reported in [1], this study will demonstrate the influence of the water concentration on steam reforming of methane/ethane mixtures on PtYSZ and Pt4K700. The kinetic data presented in both papers will be related to the characterization data, resulting in an explanation why potassium is preventing reactant competition between methane and ethane.

2. Experimental

Yttrium-stabilized zirconia (YSZ), obtained from TOSOH (TZ-8Y) was used as support and was modified with 4 wt.% potassium. About 15 g of YSZ was impregnated with 15 ml of an aqueous K_2CO_3 solution, containing 1 g of K_2CO_3 and calcined in synthetic air (30 ml min^{-1}) for 4 h at 600 °C (temperature ramp 5 °C min^{-1}).

Subsequently, a Pt loading of 1 wt.% was achieved via wet impregnation with an aqueous solution of H_2PtCl_6 (Alfa Aesar), containing 0.01 g Pt per ml. PtYSZ was calcined at 750 °C. The potassium modified samples were calcined at two different temperatures, 700 and 750 °C, respectively. Catalysts were calcined in synthetic air (30 ml min^{-1}) during 15 h (ramp 5 °C min^{-1}). Next to PtYSZ, two potassium modified catalysts were used, designated by initial potassium content (wt.%) and calcination temperature: Pt4K700 and Pt4K750.

Activity tests were carried out in a micro-reactor flow setup. The reactor consisted of a quartz tube with inner and outer diameter of respectively 4 and 6 mm. Catalyst particles with a diameter between 0.3 and 0.6 mm were used, resulting in a pressure drop around 0.1 bar, when 200 mg of catalyst was loaded between quartz wool plugs. The samples were heated to 500 °C in argon and reduced in 2.5 vol.% H_2 (Indugas 5.0)/Ar for 1 h (flow rate: 200 ml min^{-1}) before measuring the catalytic performance. No significant activity for steam reforming of methane and ethane was found for the support material YSZ at 700 °C. Also the occurrence of gas phase reactions could be excluded based on experiments with quartz particles of 0.3–0.6 mm.

Methane (Hoekloos 4.5) and ethane (Indugas 4.0) were mixed with argon (Hoekloos 5.0) to a total flow rate of 200 ml min^{-1}. Measurements were performed at 700 °C. Water was added to the gas mixtures with a Bronkhorst controlled evaporator mixer (CEM) in combination with a Liquiflow controller. To ensure constant space velocity, Ar flow was adjusted when water concentrations were changed. The product and reactant gas composition was analyzed with a Varian 3800 Gas Chromatograph equipped with two columns (Molsieve 5A and PoraPlotQ) and two TCD detectors. Water was analyzed in the PoraPlotQ column; the Molsieve column was protected against water by a PoraPlotQ pre-column and a backflush system. Argon was used as internal standard to correct for volume changes during reaction. Kinetic data were measured in random order for both PtYSZ and Pt4K700 at several methane and ethane concentrations and initial activities are reported for Pt/YSZ. To avoid any influence of catalyst deactivation on PtYSZ, a water/Ar mixture was fed at reaction conditions during 15 min between the measurements. This treatment was sufficient to fully reactivate the catalysts. The apparent reaction rates of methane and ethane per gram of catalyst were calculated based on the inlet and outlet concentrations, corrected for the volume change.

Elemental composition of the catalysts was determined with XRF on a Philips PW 1480 X-ray spectrometer. The structure of the catalysts was studied with X-ray diffraction with a Philips PW1830 diffractometer using Cu Kα radiation, $\lambda = 0.1544$ nm. XRD was performed in reflection geometry in the 2θ range between 20° and 70°. Average Pt particle size was estimated using the Scherrer equation [22]. Before XRD analysis of spent catalysts, samples were cooled to room temperature in He and exposed to air.

The transmission FT-IR CO adsorption measurements were carried out on a Bruker Vector 22 with MCT detector. A self-supporting pellet was pressed, using 15 mg of the catalyst. Before measurements the samples were reduced in 5 vol.% H_2 at 400 °C and subsequently cooled to room temperature in He. CO (Linde Gas 4.7) was absorbed at room temperature and subsequently desorbed with a heating rate of 2 °C min^{-1}.

3. Results

3.1. Catalyst characterization

It was reported in an earlier paper [1] that potassium modified catalysts activated with time on stream during reforming of methane and ethane mixtures. The apparent reaction rates initially increased and stabilized after 200–800 min of reforming of the methane and ethane mixture (a longer activation period was required with higher initial potassium content of the catalysts). The initial period of increasing activity will be referred to as "activation" in this paper. Potassium modified catalysts tested or characterized after activation are indicated with "act". Catalysts indicated with "fresh" were tested or characterized directly after calcination. The unmodified PtYSZ was tested and characterized in fresh state. PtYSZ showed initially the highest activity and slowly deactivated as a result of carbon formation [1]. After measuring the performance of PtYSZ for one specific set of experimental conditions, the catalyst was regenerated following the procedure described in [1], before the next experiment was performed.

Table 1 shows the Pt particle size for all catalysts, measured by XRD - Line Broadening. All catalysts show Pt particles between 30 and 40 nm. Calcination of potassium modified PtYSZ at 700 °C results in smaller Pt particles than calcination at 750 °C (Table 1). It is shown that Pt particles of the potassium modified Pt4K750 (calcined at 750 °C) are significantly larger that Pt particles of unmodified PtYSZ (also calcined at 750 °C) and Pt4K700 (calcined at 700 °C). It is also shown in Table 1 that Pt particle size remained unchanged during activation for both Pt4K700 and Pt4K750.

Potassium contents of fresh and used catalysts, as measured with XRF before and after steam reforming reaction, are given in Table 1. The potassium samples were initially impregnated with 4 wt.% of potassium, and it was observed that calcination temperature influences the remaining potassium content. Calcination at 700 °C leads to 2.05 wt.% of potassium, calcination at 750 °C results in only

Table 1
Pt particle size determined by XRD and potassium content determined by XRF for PtYSZ, Pt4K700act, Pt4K700fresh, Pt4K700act and Pt4K750initial.

Catalyst	Pt content (wt.%)	Average Pt particle size	Potassium content (wt.%)
PtYSZ[a]	1.04 ± 0.03	32 ± 1 nm	–
Pt4K700act	1.03 ± 0.03	30 ± 2 nm	0.90 ± 0.03
Pt4K700fresh	1.03 ± 0.03	31 ± 3 nm	2.05 ± 0.06
Pt4K750act	1.01 ± 0.03	38 ± 3 nm	0.85 ± 0.03
Pt4K750fresh	1.01 ± 0.03	38 ± 3 nm	1.60 ± 0.05

[a] Calcined at 750 °C.

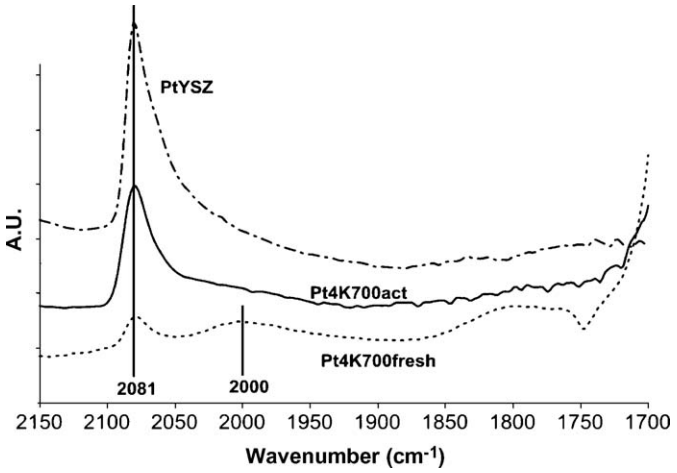

Fig. 1. FT-IR CO adsorption spectra at room temperature for PtYSZ, Pt4K700fresh and Pt4K700act.

1.6 wt.% remaining. About 50% of the potassium is lost on Pt4K700 and Pt4K750 during activation. Evaporation of potassium caused deposition of small amounts of white deposits at cold spots downstream in the reactor.

The FT-IR spectra of adsorbed CO to characterize the accessible Pt surface are shown in Fig. 1. Results of potassium modified samples are shown here for Pt4K700. For all samples 15 mg of catalyst was used.

PtYSZ, Pt4K700act and Pt4K700fresh all showed a band at 2081 cm^{-1}, attributed to CO linearly adsorbed on Pt [23]. This band had a low intensity on Pt4K700fresh. Further, a broad band around 2000 cm^{-1} was found on Pt4K700fresh, which was assigned previously to a direct ion–dipole interaction between K^+ and linear CO [24,25]. Also, a broad band around 1800 cm^{-1} was found on Pt4K700fresh, ascribed to CO coordinated in bridged position. Pt4K700act shows a larger peak at 2081 cm^{-1} compared to Pt4K700fresh, while the bands at 2000 and 1800 cm^{-1} were absent. The total integrated intensities for the different peaks are given in Table 2. It should be noted that the area of the peak around 1800 cm^{-1} on Pt4K700 fresh is less accurate as the large peak around 1700 cm^{-1} might partially contribute to its intensity. Clearly, on Pt4K700act, the peak at 2081 cm^{-1} increased by a factor 5 compared to Pt4K700fresh. The total peak area of Pt4K700act is still significantly smaller than of PtYSZ.

Table 2
Peak area between 2100 and 1900 cm^{-1} of FT-IR CO spectra of PtYSZ, Pt4K700act and Pt4K700fresh as shown in Fig. 1 (integration interval between brackets).

Catalyst	Band 2081 cm^{-1}	Band 2000 cm^{-1} (2030–1950)	Band 1800 cm^{-1} (1880–1750)
PtYSZ	0.49 (2100–2000)	–	–
Pt4K700act	0.32 (2100–2000)	–	–
Pt4K700fresh	0.06 (2090–2050)	0.07	0.28

H_2 chemisorption and TEM analysis were also carried out with all catalyst samples. However, Pt surface area was too small for H_2 chemisorption method on potassium modified samples. TEM analysis did not provide further information because of too low transmission difference between Pt and the yttrium-stabilized zirconia support.

3.2. CO desorption

Fig. 2A shows IR spectra of linearly adsorbed CO in a TPD experiment on PtYSZ. The first spectrum was taken at 35 °C (used in Fig. 1). The peak shifted to lower wave numbers with increasing temperature. This can be explained by reduced dipole–dipole coupling as a result of lower surface coverage of CO [26]. At 99 °C the peak maximum was observed at 2070 cm^{-1}. More pronounced loss of intensity was observed when heating above 99 °C and CO desorption is completed at 219 °C.

Fig. 2B shows IR spectra of linearly adsorbed CO on Pt4K700act as a function of temperature. The first spectrum was taken at 25 °C and shows linear Pt–CO adsorption at 2081 cm^{-1}. The peak was shifted to 2073 cm^{-1} when increasing temperature to 73 °C, while the peak reduced around 10% in intensity. More pronounced desorption starts already at 73 °C and is complete at 89 °C.

Fig. 3 shows the remaining CO fraction as a function of temperature obtained by integrating the peak area of the spectra shown in Fig. 2A and B, defining the initial surface coverage as 1. On Pt4K700 CO desorption started approximately 25 °C lower in temperature than on PtYSZ. Desorption of Pt4K700 is completed at 90 °C, while on PtYSZ more than 200 °C is needed to achieve total desorption. Separate TPD experiments in a dedicated TPD apparatus equipped with a mass spectrometer confirmed the difference in temperatures necessary to desorb CO from PtYSZ and Pt4K700 (not shown).

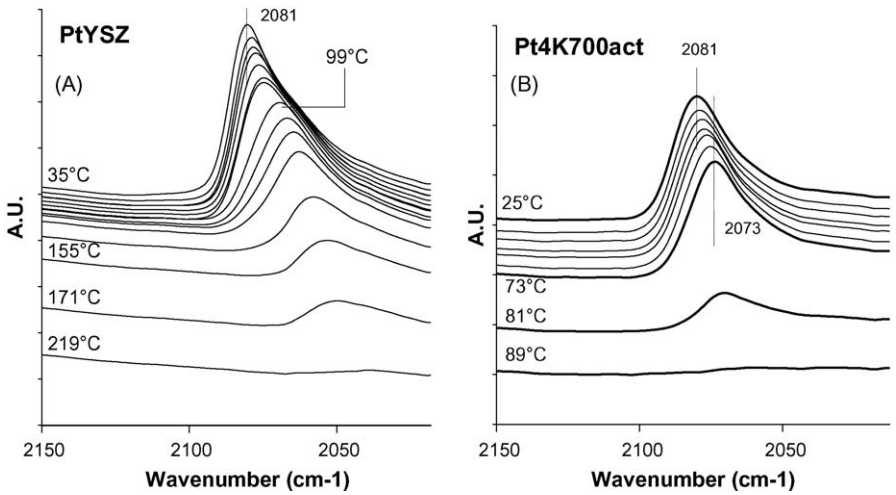

Fig. 2. CO desorption on PtYSZ (A) and Pt4K700act (B) versus temperature, monitored by transmission FT-IR spectroscopy. Heating rate was 2 °C min^{-1} and spectra are shown every 8 °C, unless indicated otherwise in A.

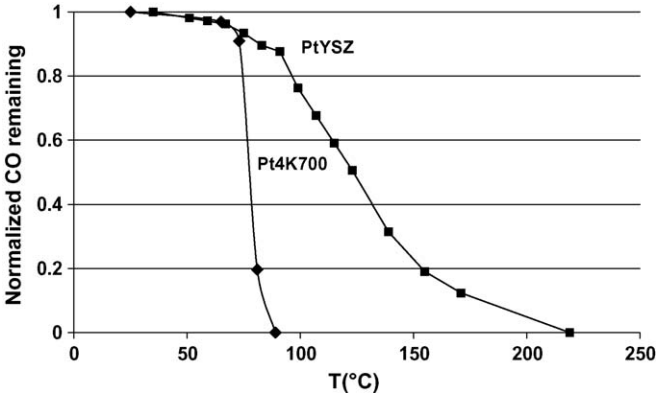

Fig. 3. Remaining normalized CO on PtYSZ and Pt4K700 as a function of temperature.

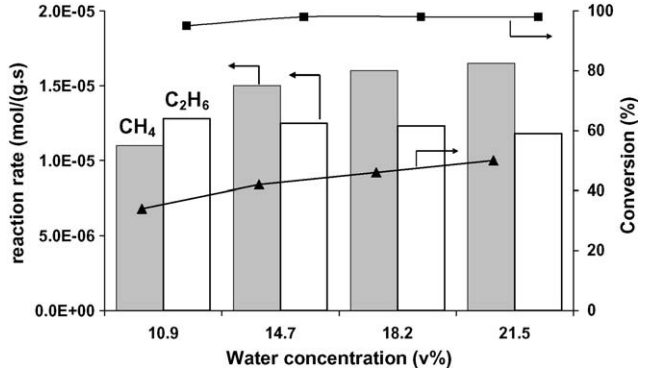

Fig. 4. Apparent reaction rates (bars) and conversions (markers) in steam reforming of a mixture of methane (▲, 4.5 vol.%) and ethane (■, 1.7 vol.%) on PtYSZ versus water concentration.

Table 3
Apparent reaction rates in mixture of methane (5 vol.%) and ethane (2.2 vol.%) for PtYSZ, Pt4K700act, Pt4K700fresh, Pt4K750act and Pt4K750fresh. Conditions: 200 mg catalyst, 200 ml min^{-1} total flow, 700 °C, water concentration 12 vol.%.

Catalyst	Reaction rate CH_4 ($\times 10^{-6}$ mol/g s)	Reaction rate C_2H_6 ($\times 10^{-6}$ mol/g s)	Ratio of reaction rates (CH_4/C_2H_6)
PtYSZ	10	12	0.83
Pt4K700act	9.4	8.5	1.11
Pt4K700fresh	2.1	1.9	1.11
Pt4K750act	7.8	7.2	1.08
Pt4K750fresh	1.1	1.0	1.10

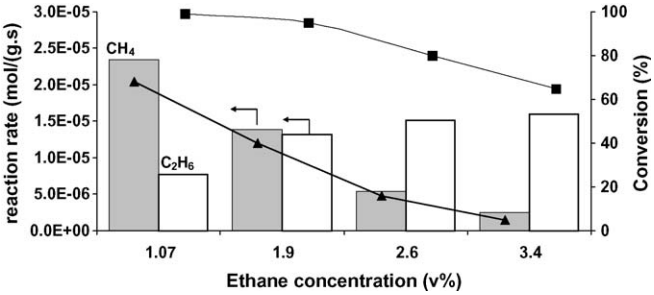

Fig. 5. Apparent reaction rates (bars) and conversions (markers) in steam reforming of a mixture of methane (▲, 4.5 vol.%) and ethane (■, 1.07–3.4 vol.%) on PtYSZ. Water/carbon ratio 1.8 and water concentration increased from left to right: 12, 15, 18 and 20 vol.%.

3.3. Catalyst performance

Table 3 shows the apparent reaction rates for methane and ethane as obtained in steam reforming experiments of a mixture of methane (5 vol.%) and ethane (2.2 vol.%) in argon. The corresponding figures and more detailed results have been published earlier [1] and are reported here for clarity reasons. As shown in Table 3, the apparent reaction rates for both methane and ethane are increasing on potassium modified catalysts with time on stream. It was also demonstrated that, depending on initial potassium content of the catalysts, stabilization of the rates was reached after 200 to 800 min of reforming of the methane and ethane mixture [1]. The experiments reported in this paper are performed on Pt4K700 after the initial activation, thus in stabilized state.

The influence of varying the water concentration on the apparent reaction rates of methane and ethane in the feed was compared on Pt4K700act and PtYSZ. The results for PtYSZ with a mixture of methane (4.5 vol.%) and ethane (1.7 vol.%) are shown in Fig. 4.

It can be seen that the apparent reaction rate of methane is increasing with increasing water concentration. Methane conversion increases from 34 to 50% when increasing the water concentration from 10.9 to 21.5 vol.%. Ethane conversion was almost complete for water concentrations of 14.7 vol.% and higher.

It should be noted that by changing the water concentration at identical hydrocarbon concentration, the water to carbon ratio changes, which could influence the apparent reaction rates as well. For this reason, additional experiments were performed to separate effects of ethane concentration and the water to carbon ratio. In the experiments shown in Fig. 5, water concentration was changed from 12 to 20 vol.%, while water/carbon ratio was kept constant at 1.8 by adjusting the ethane concentration.

Methane concentration was kept constant at 4.5 vol.% and ethane was varied between 1.07 and 3.4 vol.%. This means that the methane/ethane feed ratio was changed from 4.3 to 1.3. At an ethane concentration of 1.07 vol.%, a methane reaction rate of 2.3×10^{-5} mol/g s was found, corresponding to a conversion of 68%. Methane conversion was decreasing down to 5% when ethane concentration was increased to 3.4 vol.%. It should be noted that the methane concentration was not changed. Ethane conversion level decreased from 98% at 1.07 vol.% to 65% at 3.4 vol.%.

A second series of experiments with constant water concentration (18 vol.%) and constant water to carbon ratio (1.8) was also carried out (not shown). The ratio of methane to ethane feed was changed from 1.1 to 5.7, keeping the total carbon concentration constant. It was found that the total carbon conversion (calculated in moles of C converted) increased with increasing methane to ethane ratio (not shown).

Fig. 6 shows the influence of varying water concentration in steam reforming of a methane (4.5 vol.%) and ethane (1.7 vol.%) mixture on Pt4K700act. Water concentration was varied between 10.9 and 21.5 vol.%. In this series of experiments apparent reaction rates of methane and ethane were independent of the water concentration and thus conversions were constant, respectively 49% for ethane and 22% for methane.

4. Discussion

Potassium modified and unmodified PtYSZ show significant differences in both catalytic performance and characterization with XRD and FT-IR CO adsorption. The implications of the obtained results for steam reforming of methane and ethane will be discussed in the upcoming section. It should be noted that the typical conversions of methane and ethane are well above 10% and complying with general rules for differential experiments. Therefore, the relationship between the properties of the Pt surface and

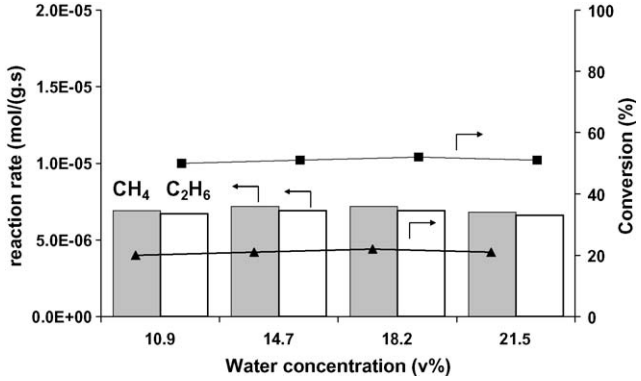

Fig. 6. Apparent reaction rates (bars) and conversions (markers) in steam reforming of a mixture of methane (■, 4.5 vol.%) and ethane (▲, 1.7 vol.%) on Pt4K700act versus water concentration.

the catalytic performance can only be qualitative. On the other hand, it is ensured that the level of conversion does not approach equilibrium in any case.

4.1. Catalyst characterization

Table 1 showed a Pt particle size of 30–40 nm for all catalysts. It was reported earlier by Juan-Juan on Ni/Al_2O_3 [8], that addition of potassium did not cause any change in Ni-particle size during calcination. However, Pt particles in Pt4K750 (38 nm) are significantly larger than Pt particles in unmodified PtYSZ (32 nm) (both calcined at 750 °C); therefore, influence of potassium on Pt sintering cannot be completely excluded based on our observations. Further, Table 1 shows larger Pt particle size at higher calcination temperature. In general, the calcination temperature affects the size of supported metal particles. High calcination temperatures result in larger metal particles due to increased surface mobility and agglomeration of particles. The difference in Pt particle size between Pt4K700act (30 nm) and Pt4K750act (38 nm) (Table 1) can explain the slightly higher reaction rates for Pt4K700act compared to Pt4K750act (Table 3). The activity per Pt surface area unit is identical within 5% for Pt4K750act and Pt4K700act, assuming hemispherical Pt particles of 38 and 30 nm, respectively. Furthermore, the rates of conversion of ethane and methane are in the same order of magnitude for PtYSZ and potassium modified catalysts under the applied conditions. However, it was observed that the apparent methane reaction rate is only 6% higher on PtYSZ than on Pt4K700act, while the apparent ethane reaction rate is 40% higher on PtYSZ (Table 3).

FT-IR characterization (Fig. 1) showed that three different CO adsorption bands were found in Pt4K700fresh: linear coordinated CO at 2081 cm^{-1}, a band around 2000 cm^{-1} due to a direct ion–dipole interaction between K^+ and linear CO [24,25], and CO coordinated in bridged position at 1800 cm^{-1} [16]. Generally, the addition of potassium can lead to an electronic modification of (small) supported metal particles, resulting in a preferred bridge coordination of CO. Interestingly, in this study the average Pt particle size is approximately 30 nm (Table 1), and still an effect of potassium on the CO FT-IR spectra is observed. Because of the large Pt particles the effect of potassium on adsorbed CO must be localized. Furthermore, potassium loss during the activation period (Table 1) led to increased intensity of CO adsorption at 2081 cm^{-1} and absence of the bands at 1800 and 2000 cm^{-1} for Pt4K700act. In addition, linear adsorbed CO on PtYSZ and Pt4K700act are at the same peak position (2081 cm^{-1}), but on PtYSZ this band was 1.5 times more intense than on Pt4K700act. Table 1 already showed that Pt particle sizes are around 30 nm for PtYSZ, Pt4K700fresh and Pt4K700act. All these observations lead to the conclusion that on Pt4K700fresh, the platinum surface is partly covered by potassium, which evaporates during the activation period. As a result the infrared bands at 1800 and 2000 cm^{-1} disappeared and the intensity at 2081 cm^{-1} significantly increased. Nevertheless, the lower amount of accessible surface sites on Pt4K700act compared to PtYSZ (Table 2) indicates that after activation still part of Pt surface in Pt4K700act is covered with potassium.

Methane and ethane reaction rates increased with a factor higher then 4 with time on stream for both potassium modified Pt catalysts. The corresponding figures were discussed in previous work [1] and are summarized in Table 3. It is shown in Table 1 that Pt particle size of Pt4K700 and Pt4K750 does not change during catalyst activation, indicating that redistribution of platinum can be excluded. It was further found that the potassium content significantly decreased during activation (shown in Table 1), indicating that potassium content and catalyst activity are related. The higher apparent reaction rates after activation combined with the increase in accessible metal surface as determined with FT-IR, suggest that on Pt4K700act hydrocarbon activation on Pt is rate determining under the present reaction conditions. Moreover, the ratio of reaction rates between methane and ethane clearly increased with potassium addition and remained constant during the activation period of Pt4K700 and Pt4K750 (Table 3). For this reason, we propose that initially two types of potassium are present on the potassium modified catalysts. Type I only blocks active Pt sites and is gradually evaporating from the metal surface during activation, as indicated by the increased number of active sites after reaction and absence of the direct Pt K^+ CO adsorption band at 2000 cm^{-1} and bridged CO band at 1800 cm^{-1} in Pt4K700act. The second type of potassium proved to be more stable, as the potassium content did not change during reaction between 20 and 85 h of time on stream, after activation had taken place [1]. The fact that potassium of type II is not lost, suggests a stronger interaction with either the YSZ support material or with Pt. It is proposed that the stable type of potassium influences the ratio of reaction rates of methane and ethane by modifying the surface properties of Pt or the support.

4.2. CO desorption in FT-IR-TPD

CO temperature programmed desorption has been widely studied [27] and used in investigation of catalytic systems [28,29]. TPD studies in IR spectroscopy have been used earlier by Visser et al. [15]. The intention of their experiments was to relate observations of CO adsorption strength to reactivity of hydrocarbons found in kinetic experiments, as reported earlier in literature on hydrogenolysis, hydrogenation and oxidation reactions [13–15,21].

Here, it was found in FT-IR and CO desorption experiments that CO release from the Pt surface occurred at lower temperature when potassium was added (Figs. 2 and 3). It was also observed that CO desorption was completed at lower temperature on Pt4K700 compared to PtYSZ (Fig. 3). The data convincingly show weaker CO bonding as a result of the addition of potassium.

Kuriyama et al. [17,30] and Derrouiche et al. [16,31] also investigated interaction of CO on potassium modified Pt/Al_2O_3 with FT-IR. Derrouiche reported IR bands on 2.9 wt.% Pt/10 wt.% K/Al_2O_3 located at 2074, 1990 and 1795 cm^{-1}, comparable to our results in Fig. 1. The intensity of the peak of linear CO on Pt decreased significantly as a result of potassium addition, in agreement with our results in Fig. 1. TPD experiments by Kuriyama showed complete CO desorption at about 150 °C lower temperature on potassium modified 10 wt.%K/2 wt.%Pt/Al_2O_3 as compared to Pt/Al_2O_3, clearly showing weaker adsorption of CO. This is in agreement with our results in Fig. 3, showing a similar difference of

130 °C in temperature is needed to achieve complete desorption on Pt4K700 versus PtYSZ.

Derrouiche et al. determined the heat of adsorption with the Adsorption Equilibrium Infrared method (AEIR) on 2.9 wt.% Pt/10 wt.% K/Al_2O_3 [16] and reported a significant decrease in heat of adsorption of linear CO species and a strong increase in heat of adsorption for bridged CO species as a result of potassium addition to Pt. This completely agrees with our results in Fig. 3, showing a weaker interaction for linear CO species at 2081 cm^{-1} on Pt4K700act, which had only linear CO species present on the surface (Fig. 1). Obviously, the C–O stretch frequency, which is identical for PtYSZ and Pt4K700act, does not reflect the Pt–CO bond strength.

Bengaard et al. [32] observed weaker adsorption of hydrocarbons on Ni catalysts after adding potassium: a strong decrease in methane adsorption was found when potassium was added, resulting in slow hydrogen–deuterium exchange for methane compared to the unmodified catalyst Ni catalyst. Cassuto et al. found more loosely bonded ethylene on potassium modified platinum surfaces [33]. Summarizing the results in literature, it is claimed that hydrocarbon adsorption on Pt can be weakened by addition of potassium to Pt or Ni catalysts. We propose, based on our results on CO desorption, that weakening of hydrocarbon adsorption occurs when modifying PtYSZ with potassium. The effects on kinetics on PtYSZ and Pt4K700 will be discussed below.

4.3. Steam reforming reaction mechanism on PtYSZ

For methane reforming, Wei and Iglesia [34,35] proposed dissociative adsorption as the rate determining step in methane activation: $CH_{4,\ gas} \rightarrow CH_{3(ads)} + H_{(ads)}$. This means that the hydrocarbon surface coverage is low and reaction proceeds rapidly after dissociation of methane. Reaction to CO occurs as soon as the carbon atom is completely dehydrogenated. In literature, debate exists about the activation of water on Pt catalysts in steam reforming at high temperature: several sources claim a bi-functional mechanism for reforming reactions on Pt, proposing hydrocarbon activation on the Pt atoms and water activation on the support [36–38]. On the other hand, Wei and Iglesia [34,39,40] argued that water activation is a relatively fast step, implying that the question on which sites water is activated is not relevant for reaction kinetics.

To the best of our knowledge no detailed mechanism has been reported for steam reforming of ethane, but ethane hydrogenolysis has been investigated in detail on Pt and Ni catalysts [41–43]. It was reported that activity trends in steam reforming and ethane hydrogenolysis are comparable on supported Ni catalysts [9], suggesting similar mechanisms for ethane activation in both reactions. In hydrogenolysis, activation of ethane on Pt or Ni takes place through dissociative adsorption on the surface (5), creating adsorbed ethylidyne and an hydrogen atom [41–43]:

$$C_2H_6 \rightarrow CH_3CH_{2(ads)} + H_{(ads)} \quad (5)$$

$$CH_3CH_{2(ads)} \rightarrow CH_{2(ads)} + CH_{3(ads)} \quad (6)$$

$$CH_3CH_{2(ads)} \rightarrow CH_2CH_{2(ads)} + H_{(ads)} \quad (7a)$$

$$CH_3CH_{2(ads)} \rightarrow CH_3CH_{(ads)} + H_{(ads)} \quad (7b)$$

$$CH_3CH_{(ads)} \rightarrow CH_3C_{(ads)} + H_{(ads)} \quad (7c)$$

Two pathways are possible after formation of the CH_3CH_2 fragment: (i) the CH_3CH_2 fragment can either split into a CH_3 and a CH_2 fragment after adsorption (6) or (ii) further abstraction of hydrogen atoms can occur (7a + 7b + 7c) [41,42]. Both processes require additional empty surface sites. The C–C splitting is favored for the CH_3CH_2 fragment on Pt [41,42]. After C–C splitting, further dehydrogenation of CH_x can occur, similar to the mechanism for methane, and subsequent conversion to CO is possible as explained above.

If further abstraction of hydrogen atoms on CH_3CH_2 fragments occurs (7a + 7b + 7c), much less reactive surface intermediates are formed, occupying the Pt sites. It is claimed that CCH_3-fragments on the Pt surface are the most stable species that block the Pt surface sites [41,42]. Very low reactivity of the CCH_3-species on the surface was also reported by Anderson and Choe [44] in ethylene dehydrogenation on platinum.

Our study focused on steam reforming of methane/ethane mixtures, requiring activation of both hydrocarbons on PtYSZ. Competition between methane and ethane in steam reforming was observed on PtYSZ (Fig. 5). This leads to the proposition that methane and ethane are indeed activated on the same Pt sites. The water concentration was also found to influence reaction rates in ethane/methane mixtures on PtYSZ as shown in Fig. 4: higher apparent reaction rates with increasing water concentration show that water activation on this catalyst is a limiting factor. This suggests that the Pt surface is highly covered with fragments originating from dissociative adsorption of methane and/or ethane.

The results in Fig. 5 show that the relative increase of the apparent reaction rates with higher water concentration is smaller than the decreasing effects caused by the increasing ethane concentration. This is confirmed by the total molar carbon conversion in the experiments of Fig. 5, as shown in Table 4 (reaction of methane counts for one carbon atom converted, while ethane counts for two atoms). With higher ethane concentration in the feed, the percentage of carbon converted is decreasing, even when the water concentration is increased proportionally. Fig. 5 thus shows that the methane reaction rate strongly decreased if more ethane is present, and that high methane conversions are only possible if ethane is converted completely, confirming competition between methane and ethane on the platinum surface.

Furthermore, in Fig. 5, ethane conversion decreased from 98% at 1.07 vol.% to 65% at 3.4 vol.%, implying that the apparent reaction order in ethane is smaller than 1. This indicates a self-poisoning effect due to blocking of active sites by ethane fragments. The creation of stable C_2 intermediates as reported by Cortright et al. [41,42] on the Pt surface could be a reason for limited adsorption and activation of methane at higher ethane concentrations (Fig. 5). Higher ethane concentrations create more stable C_2-fragments on the Pt surface, leaving a lower percentage of the active sites open for methane dissociation and reaction to CO and H_2. It is concluded that ethane induces a high surface coverage of C_2H_y fragments and water activation becomes the rate limiting step in mixtures of methane and ethane on PtYSZ.

4.4. Steam reforming reaction mechanism on Pt4K700

The addition of potassium could affect the apparent reaction rates of methane and ethane in steam reforming in two ways: potassium either influences the activation of water or modifies the activation of the hydrocarbons, methane and ethane. In literature it is stated that potassium can indeed enhance water activation on

Table 4
Total number of carbon atoms converted in the experiments shown in Fig. 5, [CH4] = 4.5 vol.%, H_2O/C ratio 1.8.

Water (vol.%)	12	15	18	20
Ethane (vol.%)	1.07	1.9	2.6	3.4
Total C conversion ($\times 10^{-5}$ mol/g s)	3.1	4.0	3.6	3.5
Carbon converted (%)	46.7	48.2	37.1	31.0

the support [45,46], but as indicated earlier, there is no agreement in literature on the kinetic relevance of water activation on the support on steam reforming [34–38,40].

In our experiments with Pt4K700, it was observed that a changing water concentration had no influence on apparent reaction rates for both methane and ethane (Fig. 6), in contrast to PtYSZ (Fig. 4). With the addition of potassium to PtYSZ, the competition between ethane and methane was diminished, as reported in an earlier paper [1]. First order kinetics in methane and ethane was reported, indicating low surface coverage of both hydrocarbons, even in mixtures of methane and ethane. The apparent first order in both methane and ethane suggests that hydrocarbon activation on Pt is the limiting step on Pt4K700 and activation of water is not kinetically relevant, as observed in Fig. 6. The conclusion that hydrocarbon activation is rate limiting on Pt4K700 is also in agreement with the observation that increasing the number of accessible Pt sites with TOS (Fig. 1) is accompanied by an increase in catalytic activity.

In an earlier paper [1], a lower activity was reported for the potassium modified catalysts during steam reforming of the single hydrocarbons ethane and methane, as compared to the unmodified Pt/YSZ catalyst. For methane the activity decreased by 60%, while for ethane reaction rate decreased by 33%. The IR experiments in this work indicate that potassium weakens the interaction with methane and ethane, leading to lower surface coverages of methane and ethane. The lower surface coverages can explain the observed lower reaction rates of methane and ethane on Pt4K700 as compared to PtYSZ.

Interestingly, contrary to the rate limiting step found for Pt/YSZ, the rate limiting step of hydrocarbon activation on Pt4K700 is well in agreement with the mechanism proposed by Wei and Iglesia [34,35,40]; competition effects as observed on PtYSZ, leading to high surface coverage, were eliminated on potassium modified catalysts. In conclusion, our results show that adsorption for both ethane and methane was reduced on potassium modified PtYSZ. Blocking effects by ethane as observed on PtYSZ could be eliminated by reducing the alkane adsorption strength. However, this also resulted in reduced adsorption of methane, leading to lower reactivity for both hydrocarbons.

5. Conclusion

Potassium modification of PtYSZ strongly influenced the conversion and rate determining steps in methane and ethane in steam reforming. Water activation is the rate determining step on PtYSZ, resulting in high surface coverage of hydrocarbon fragments during steam reforming of mixtures of methane and ethane. This led to blocking of active sites by ethane fragments and consequently low conversion of methane. If potassium is added to the catalyst, hydrocarbon activation on Pt is rate determining, resulting in low surface coverage of methane and ethane. As a result, competition effects of methane and ethane diminished on potassium modified PtYSZ, enabling simultaneous conversion of methane and ethane. The weaker interaction of the hydrocarbons with the Pt surface due to potassium addition is also reflected in the lower adsorption strength of CO as found with CO-FT-IR-TPD.

References

[1] P.O. Graf, B.L. Mojet, L. Lefferts, Applied Catalysis A: General 346 (2008) 90.
[2] P.O. Graf, B.L. Mojet, J.G. van Ommen, L. Lefferts, Applied Catalysis A: General 332 (2007) 310–317.
[3] D.L. Trimm, Catalysis Today 37 (1997) 233.
[4] J.H. Bitter, W. Hally, K. Seshan, J.G. van Ommen, J.A. Lercher, Catalysis Today 29 (1996) 349–353.
[5] J.H. Bitter, K. Seshan, J.A. Lercher, Journal of Catalysis 171 (1997) 279.
[6] M.E.S. Hegarty, A.M. O'Connor, J.R.H. Ross, Catalysis Today 42 (1998) 225.
[7] A.M. O'Connor, J.R.H. Ross, Catalysis Today 46 (1998) 203.
[8] J. Juan-Juan, M.C. Roman-Martinez, M.J. Illan-Gomez, Applied Catalysis A: General 301 (2006) 9–15.
[9] J.R. Rostrup-Nielsen, Journal of Catalysis 31 (1973) 173.
[10] J. Sehested, Catalysis Today 111 (2006) 103–110.
[11] J.W. Snoeck, G.F. Froment, M. Fowles, Industrial and Engineering Chemistry Research 41 (2002) 3548–3556.
[12] D.L. Trimm, Catalysis Today 49 (1999) 3.
[13] B.L. Mojet, J.T. Miller, D.E. Ramaker, D.C. Koningsberger, Journal of Catalysis 186 (1999) 373–386.
[14] M.K. Oudenhuijzen, J.A. Van Bokhoven, D.E. Ramaker, D.C. Koningsberger, Journal of Physical Chemistry B 108 (2004) 20247–20254.
[15] T. Visser, T.A. Nijhuis, A.M.J. Van Der Eerden, K. Jenken, Y. Ji, W. Bras, S. Nikitenko, Y. Ikeda, M. Lepage, B.M. Weckhuysen, Journal of Physical Chemistry B 109 (2005) 3822–3831.
[16] S. Derrouiche, P. Gravejat, B. Bassou, D. Bianchi, Applied Surface Science 253 (2007) 5894–5898.
[17] M. Kuriyama, H. Tanaka, S.-i. Ito, T. Kubota, T. Miyao, S. Naito, K. Tomishige, K. Kunimori, Journal of Catalysis 252 (2007) 39–48.
[18] E.L. Garfunkel, J.E. Crowell, G.A. Somorjai, Journal of Physical Chemistry 86 (1982) 310–313.
[19] P.A.J.M. Angevaare, H.A.C.M. Hendrickx, V. Ponec, Journal of Catalysis 110 (1988) 11–17.
[20] H.P. Bonzel, Surface Science Reports 8 (1988) 43–125.
[21] A.Y. Stakheev, Y. Zhang, A.V. Ivanov, G.N. Baeva, D.E. Ramaker, D.C. Koningsberger, Journal of Physical Chemistry C 111 (2007) 3938–3948.
[22] H. Borchert, E.V. Shevchenko, A. Robert, I. Mekis, A. Kornowski, G. Grubel, H. Weller, Langmuir 21 (2005) 1931–1936.
[23] S.D. Jackson, B.M. Glanville, J. Willis, G.D. McLellan, G. Webb, R.B. Moyes, S. Simpson, P.B. Wells, R. Whyman, Journal of Catalysis 139 (1993) 221–233.
[24] M.J. Kappers, J.T. Miller, D.C. Koningsberger, Journal of Physical Chemistry 100 (1996) 3227–3236.
[25] A.Y. Stakheev, E.S. Shpiro, N.I. Jaeger, G. Schulz-Ekloff, Catalysis Letters 32 (1995) 147–158.
[26] P. Hollins, J. Pritchard, Progress in Surface Science 19 (1985) 275–349.
[27] D.A. King, 1 ed., Utrecht, Netherlands, 1975, Surf. Sci. (Netherlands) Vol.47, pp. 384-402.
[28] A.M. de Jong, J.W. Niemantsverdriet, Vacuum 41 (1990) 232–233.
[29] D.L.S. Nieskens, A.P. Van Bavel, J.W. Niemantsverdriet, Surface Science 546 (2003) 159–169.
[30] Y. Minemura, M. Kuriyama, S.-i. Ito, K. Tomishige, K. Kunimori, Catalysis Communications 7 (2006) 623–626.
[31] P. Pillonel, S. Derrouiche, A. Bourane, F. Gaillard, P. Vernoux, D. Bianchi, Applied Catalysis A: General 278 (2005) 223–231.
[32] H.S. Bengaard, J.K. Norskov, J. Sehested, B.S. Clausen, L.P. Nielsen, A.M. Molenbroek, J.R. Rostrup-Nielsen, Journal of Catalysis 209 (2002) 365–384.
[33] A. Cassuto, S. Schmidt, M. Mane, Surface Science 284 (1993) 273–280.
[34] J.M. Wei, E. Iglesia, Journal of Catalysis 225 (2004) 116.
[35] J.M. Wei, E. Iglesia, Journal of Physical Chemistry B 108 (2004) 4094.
[36] K. Nagaoka, K. Seshan, K. Aika, J.A. Lercher, Journal of Catalysis 197 (2001) 34.
[37] K. Takanabe, K.-i. Aika, K. Inazu, T. Baba, K. Seshan, L. Lefferts, Journal of Catalysis 243 (2006) 263–269.
[38] B. Matas Guell, I. Babich, K. Seshan, L. Lefferts, Journal of Catalysis 257 (2008) 229–231.
[39] J. Wei, E. Iglesia, Journal of Physical Chemistry B 108 (2004) 4094–4103.
[40] J.M. Wei, E. Iglesia, Physical Chemistry Chemical Physics 6 (2004) 3754.
[41] R.D. Cortright, R.M. Watwe, J.A. Dumesic, Journal of Molecular Catalysis A: Chemical 163 (2000) 91–103.
[42] R.D. Cortright, R.M. Watwe, B.E. Spiewak, J.A. Dumesic, Catalysis Today 53 (1999) 395.
[43] M.C. McMaster, R.J. Madix, Surface Science 275 (1992) 265–280.
[44] A.B. Anderson, S.J. Choe, Journal of Physical Chemistry 93 (1989) 6145–6149.
[45] F. Frusteri, S. Freni, V. Chiodo, L. Spadaro, O. Di Blasi, G. Bonura, S. Cavallaro, Applied Catalysis A: General 270 (2004) 1–7.
[46] D. Sutton, B. Kelleher, J.R.H. Ross, Fuel Processing Technology 73 (2001) 155–173.